



This is a repository copy of *In-situ U-value measurements of typical building envelopes in a severe cold region of China: U-value variations and energy implications.*

White Rose Research Online URL for this paper:

<https://eprints.whiterose.ac.uk/219344/>

Version: Accepted Version

Article:

Yu, J. orcid.org/0000-0001-5567-5716, Chang, W.-S., Zhang, R. et al. (3 more authors) (2024) In-situ U-value measurements of typical building envelopes in a severe cold region of China: U-value variations and energy implications. *Energy and Buildings*, 324. 114947. ISSN 0378-7788

<https://doi.org/10.1016/j.enbuild.2024.114947>

© 2024 The Authors. Except as otherwise noted, this author-accepted version of a journal article published in *Energy and Buildings* is made available via the University of Sheffield Research Publications and Copyright Policy under the terms of the Creative Commons Attribution 4.0 International License (CC-BY 4.0), which permits unrestricted use, distribution and reproduction in any medium, provided the original work is properly cited. To view a copy of this licence, visit <http://creativecommons.org/licenses/by/4.0/>

Reuse

This article is distributed under the terms of the Creative Commons Attribution (CC BY) licence. This licence allows you to distribute, remix, tweak, and build upon the work, even commercially, as long as you credit the authors for the original work. More information and the full terms of the licence here:

<https://creativecommons.org/licenses/>

Takedown

If you consider content in White Rose Research Online to be in breach of UK law, please notify us by emailing eprints@whiterose.ac.uk including the URL of the record and the reason for the withdrawal request.



eprints@whiterose.ac.uk
<https://eprints.whiterose.ac.uk/>

1 **In-situ U-value Measurements of Typical Building Envelopes in a Severe Cold**
2 **Region of China: U-value Variations and Energy Implications**

3
4 Jiaqi Yu^a, Wen-Shao Chang^b, Ruinan Zhang^{c,d}, Yu Dong^{c,d*}, Haoyu Huang^e, Tsung-Hsien Wang^a

5 *^aSchool of Architecture, University of Sheffield, Sheffield S10 2TN, United Kingdom;*

6 *^bLincoln School of Architecture and the Built Environment, University of Lincoln, Lincoln LN6 7TS, United Kingdom;*

7 *^c School of Architecture and Design, Harbin Institute of Technology, Harbin, 150001, China*

8 *^d Key Laboratory of Cold Region Urban and Rural Human Settlement Environment Science and Technology, Ministry of Industry and Information Technology,*
9 *Harbin, 150001, China*

10 *^eSchool of Engineering, Newcastle University, Newcastle NE1 7RU, United Kingdom*

11 ** Corresponding author*

12
13 **ABSTRACT**

14 Building energy consumption in the severe cold regions of China is an important consideration in
15 building energy conservation because of the high amount of energy consumed by heating. As an
16 important thermal parameter, the thermal transmittance (U-value) of building envelopes can directly
17 affect the operational energy consumption of buildings. Understanding the U-values of buildings in
18 severe cold regions is important to predict building energy accurately. However, the U-values of
19 envelopes fluctuate constantly due to environmental impacts. Therefore, this study aimed to
20 examine the influence of dynamic U-values on building energy efficiency. To achieve this, this study
21 focused on the in-situ measurement of the U-values of two typical building envelopes in Harbin
22 from winter to summer in 2023 to determine the average and dynamic U-values of the tested
23 envelope, comprising a brick envelope and reinforced concrete (RC) envelope. The building energy
24 simulation results based on theoretical U-values were compared with the measured average and
25 dynamic U-values of the tested envelopes. The findings revealed that the fluctuations in the U-
26 values were significant. In the dynamic U-values of tested brick and RC envelopes, the U-values in
27 winter were 159.8% and 30.8% higher than those in summer, respectively. Furthermore, the
28 dynamic U-values significantly influenced heating energy consumption, with an increase of up to
29 15.9%.

30
31 **Keywords: In-situ U-value measurement; HFM method; Dynamic U-value; Residence energy**
32 **consumption; Building envelopes**

Nomenclature

RC	Reinforced concrete
HDD18	Heating design days (base temperature 18 °C) [°C · d]
CDD26	Cooling design days (base temperature 26 °C) [°C · d]
HFM	Heat flow meter
RHS-HFM	Removing the heat storage effect - heat flow meter
RH	Relative humidity [%]
U	Thermal transmittance [W/(m ² · K)]
R	Thermal resistance [(m ² · K)/W]
D	Thickness of the material [mm]
λ	Thermal conductivity of the material [W/(m · K)]
q	Heat flow density [W/m ²]
T	Temperature [K]
ΔT	Temperature difference between indoor and outdoor environment [K]
G	Total solar energy transmittance

Subscripts

mea	Measured
theo	Theoretical
se	External surface of the envelope
si	Internal surface of the envelope
out	Outdoor environment
in	Indoor environment
max	Maximum value
min	Minimum value
period, i	In the ith period
N	Total measurement duration
n	Number of periods comprising total duration of measurement

45
46
47
48
49
50
51
52
53
54
55
56
57
58
59
60
61

1 Introduction

The construction industry is an important contributor to energy consumption in all sectors across the world [1-3]. According to the International Energy Agency, the construction industry accounts for 36% of final energy use [4]. China's building energy use comprises one billion tons of standard coal, representing 21.7% of the country's total energy use [5]. In China, the building energy use in severe cold regions is enormous because of centralised heating systems with long-term heating periods [6]. For example, as a major city in a severe cold region, Harbin has 5 months per year when the centralised heating systems are activated [7]. The heating energy consumption in severe cold regions accounted for 24.1% of the total energy use of the construction industry in 2010 [8]. The building sector is regarded as one of the most cost-efficient fields for reducing energy consumption [9]. Consequently, numerous researchers have concentrated on developing building energy simulations to precisely manage energy usage and ensure a comfortable indoor environment for occupants [10-14].

As an important thermal parameter of the envelope, the U-value, also called thermal transmittance, directly affects building energy simulations, particularly cooling and heating energy use simulations [15-17]. Well-insulated envelopes have low U-values while poorly insulated envelopes have high U-values. In recent years, there has been notable growth in building energy simulation studies focusing on the effects of U-values on operational energy consumption [16, 18-21]. For example, Fernandes et al. used EnergyPlus to study the impact of U-value variations on building energy use in the Mediterranean region [20]. Their results revealed that an increase in the U-values can decrease the operational energy consumption in the lower northern latitudes. Building energy consumption was reduced by 20% when the U-value of envelopes increased from 0.15 to 0.3 W/(m² · K) in Alexandria, Greece. Conversely, at higher northern latitudes, the operational energy consumption decreases with decreasing U-value. The operational energy consumption increased by 15% when the U-value of envelopes increased from 0.25 W/(m² · K) to 0.5 W/(m² · K) in Izmir. These studies indicate that different U-values significantly affect the operational energy simulation results. Therefore, the precise determination of U-values is essential for accurately predicting operational energy consumption.

In most existing building energy simulation studies, the U-value parameters are set to theoretical U-values rather than measured U-values [22-25]. The theoretical U-values of the envelopes can be calculated based on the thickness and thermal conductivity of every layer within building envelopes according to the ISO 6946 standard [26]. In an actual environment, several environmental factors can influence the thermal conductivity of building materials and the U-values of envelopes, most notably the atmospheric temperature and relative humidity (RH) [17, 24, 27, 28]. Thus, there is a discrepancy between the theoretical and actual U-values [25]. To obtain accurate U-values for envelopes in an actual environment, studies have conducted in-situ U-value measurements [29-32]. Four in-situ measurement methods have been used in past studies: heat flow meter (HFM), simple hot box-heat flow meter, thermometry, and quantitative infrared thermography method [17, 33-36]. Among these, the HFM method is a common method which necessitates the installation of a set of U-value measurement instruments in a tested room [37]. The standardised HFM method is governed by the ISO 9869-1 and ASTM C1155 standards [38, 39]. Numerous researchers have applied this

106 method to measure the average U-values of building envelopes [29, 30, 32, 33, 40-46]. These results
107 revealed a large discrepancy between the theoretical and measured average U-values of the building
108 envelopes. For example, O'Hegarty investigated seven concrete walls with different structures using
109 in-situ U-value measurements. The results showed that The measured U-values of the four tested
110 walls were more than twice the theoretical U-values [27].

111
112 However, building energy simulations that involve inputting a single U-value cannot accurately
113 reflect the real situation, even if the input U-value is the measured average U-value [25]. As
114 environmental factors vary constantly, the hygrothermal behaviour of building materials is always
115 changing, causing U-values to fluctuate [47]. The hygrothermal behaviour of building materials
116 refers to the changes in their physical properties due to the absorbing, storing and releasing of heat,
117 liquefying and vaporising of moisture [48]. This behaviour is associated with the microstructure of
118 the building materials [49]. The microstructures of conventional building materials are inorganic
119 and porous structures [50]. Changes in air temperature and RH affect the hygrothermal behaviour
120 of building materials with different material porosities, including changes in the moisture content
121 and internal temperature of materials [51]. Such changes affect the thermal conductivities of
122 building materials [52, 53]. This results in dynamic U-values of the envelopes, as the U-value is
123 positively correlated with the thermal conductivity of building materials [54]. Thus, compared to
124 the theoretical and measured average U-values, the dynamic U-values were closer to the real
125 conditions of the envelopes.

126
127 Several researchers have realised the existence and impact of dynamic U-values [55-57]. Dynamic
128 U-values show that the thermal properties of building envelopes are unstable [24, 25]. However,
129 few researchers have realised the impact of dynamic U-values on operational energy. Bruno and
130 Bevilacqua applied WUFI software to simulate the dynamic U-values of three conventional walls
131 in a Mediterranean climate [16]. The results revealed that the monthly variation in U-values was
132 significant. The operational energy consumption results obtained from the dynamic U-values were
133 higher than those obtained from the average U-values. This confirms that inputting dynamic U-
134 values can significantly impact the operational energy simulation results. Notably, no studies have
135 measured the dynamic U-values or used them for operational energy simulations.

136
137 Compared to a mild climate region, the energy conservation of building heating systems in a severe
138 cold region is a noteworthy issue, as a cold region consumes more than three times as much heating
139 energy as a temperate region [58, 59]. The dynamic U-values of envelopes in a severe cold region
140 may significantly influence operational energy consumption. There are two existing research gaps
141 in dynamic U-values and operational energy consumption in the severe cold region of China: (1)
142 existing dynamic U-value data are not supported by actual measured data. Although many
143 researchers have conducted in-situ U-value measurements, they have focused on average U-values
144 rather than dynamic U-values [30, 44, 46, 60-62]. (2) Limited related studies focused on climate
145 zone where buildings consume more energy, such as severe cold zone. Compared to mild climate
146 zone, energy conservation of building heating system in severe cold zone is a noteworthy issue.
147 Severe cold zone consumes more than three times as much heating energy as temperate zone [58,
148 59].

149

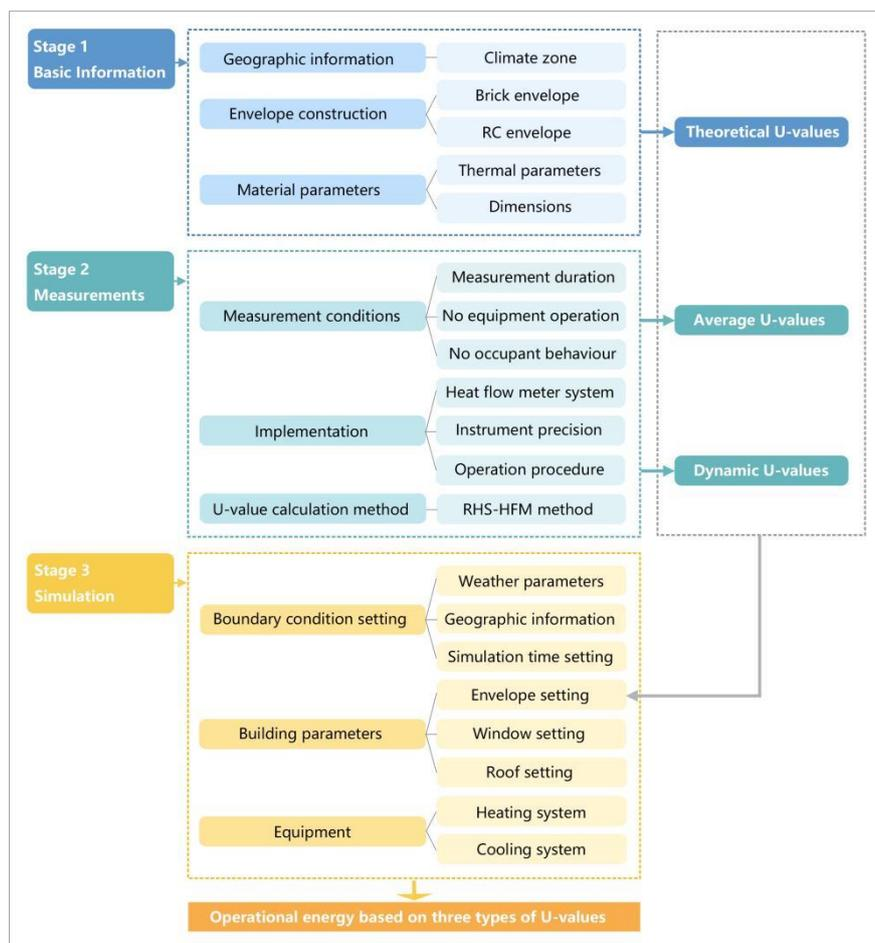
150 The novelty of this paper is studying the influences of measured dynamic U-values on simulation
 151 results of operational energy efficiency in severe cold regions of China. The study results expect to
 152 reduce the gap between building energy simulations and actual energy consumption by inputting
 153 the measured dynamic U-values. In-situ U-value measurements of typical brick and reinforced
 154 concrete (RC) envelopes were conducted from winter to summer in Harbin, China. The
 155 measurement method is according to the HFM method in ISO 9869-1 [38]. The measured average
 156 and dynamic U-values were obtained. The theoretical, average, and dynamic U-values were applied
 157 to the operational energy simulation. Finally, the operational energy results simulated by the three
 158 types of U-values were compared to quantitatively study the influence of the dynamic U-values of
 159 typical envelopes on the operational energy efficiency in a severe cold region of China.

160

161 2 Methods

162

163 The framework of this study is shown in Figure 1. The theoretical U-values of the tested envelopes
 164 were calculated based on the basic information of the tested envelopes and the average and dynamic
 165 U-values of the tested envelopes were obtained from the in-situ U-value measurements. Finally, the
 166 operational energy simulation results based on three types of U-values were compared.



167

168

169

170

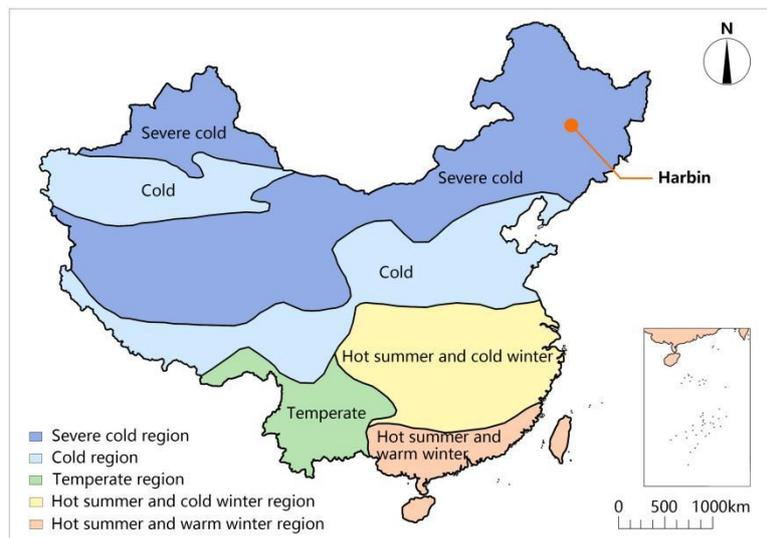
Fig. 1. Framework of the study

171 2.1. Weather Region of Harbin

172

173 Two typical external envelopes were tested in two residential buildings in Harbin, China. Harbin is
 174 located at latitude 45.7567°N and longitude 126.6424°E with a monsoon-influenced humid
 175 continental climate (Köppen climate classification: Dwa) [63]. Under the Code for Thermal Design
 176 of Civil Buildings in China (GB 50176-2016), China is divided into five main climate regions, and
 177 Harbin is situated in a severe cold region, as shown in Figure 2 [7]. Harbin is one of the major cities
 178 in the severe cold region of China, with a population of nearly 10 million [64]. The climate in Harbin
 179 varies greatly in different seasons. The difference between the average January and July
 180 temperatures in Harbin can be up to 40 °C [7]. This obvious temperature fluctuation is beneficial
 181 for observing and studying the fluctuation of U-values under different temperature conditions. In
 182 addition, Harbin has a large population, and it is significant to study building energy consumption
 183 in this region. Therefore, Harbin was chosen as the case city. Detailed meteorological information
 184 for Harbin is presented in Table 1.

185



186

187

188

Fig. 2. Five climate regions of China.

189 Table 1. Meteorological information of Harbin

Parameter	Value
Climate region	Severe Cold Region
Average annual temperature	3.6 °C
Average temperature of January	-16.9 °C
Average temperature of July	23.8 °C
Number of days with average daily temperatures below 5 °C	167 days in a year
Heating design days (base temperature 18 °C) (HDD18)	5032 °C · d
Cooling design days (base temperature 26 °C) (CDD26)	14 °C · d

Data source: the Code for Thermal Design of Civil Building (GB 50176-2016) [7]

190

191 2.2. Tested envelopes

192

193 The two residential buildings tested were constructed in the 1980s and the 2010s using brick and
194 RC constructions, respectively. The building envelopes of these two structures have been widely
195 applied in the severe cold regions of Northeast China in recent decades. Before the 1990s, clay
196 bricks were the principal building material in China. Clay is a non-renewable resource obtained
197 from arable land that has caused the reduction and depletion of land resources; thus, the use of clay
198 bricks was gradually restricted in the 2000s. Since the 2000s, concrete has replaced clay bricks as
199 the primary building material in China [65].

200

201 Numerous brick buildings are built over three decades in Northeast China. The insulation
202 performances of the envelopes are affected by material ageing in these buildings. According to
203 existing studies, the measured U-values of envelopes of brick buildings around 30 years old were
204 around twice the theoretical U-values of these envelopes, whereas the measured U-values of
205 envelopes of brick buildings around 15 years old were around 1.3 times as much as the theoretical
206 U-values of these envelopes [66]. It means that the actual insulation performance is lower than the
207 expected insulation performance in older brick buildings.

208

209 Photographs of the test rooms and the room dimensions are shown in Figure 3. Both test rooms were
210 bedrooms with one exterior envelope and one exterior window. The room and window dimensions
211 of two test rooms were slightly different. This difference could have an effect on indoor temperature.
212 According to the HFM method [38], the measured U-values were calculated by measuring the
213 indoor and outdoor temperatures and heat flow density. Although dimensional factors affecting
214 indoor temperature, they were not considered in the measured U-value calculation in this study.
215 Case A was the brick envelope in test room A and Case B was the RC envelope in test room B. The
216 test envelopes were multilayered. Detailed information on Cases A and B is presented in Table 2.

217

218 The theoretical U-values of the tested envelopes were obtained in accordance with ISO 6946 [26].
219 Using this method, the theoretical U-values can be estimated using the envelope parameters, as
220 shown in Eqs.(1-2):

221

$$U = 1/(R_{se} + R_{si} + R_1 + R_2 + R_3 + \dots + R_N) [W/(m^2 \cdot K)] \quad (1)$$

$$R = D/\lambda [(m^2 \cdot K)/W] \quad (2)$$

222

223 where R_{se} is thermal resistance of exterior surface, R_{si} is thermal resistance of interior surface,
224 $R_1 + R_2 + R_3 + \dots + R_N$ is the sum of thermal resistance of every layer within the envelope, D is
225 the thickness of the building material, and λ is the thermal conductivity of the building material.
226 In this study, R_{se} was estimated as $0.04 (m^2 \cdot K)/W$ and R_{si} was estimated as $0.13 (m^2 \cdot K)/W$
227 according to the ISO 6946 [26]. Based on the envelope parameters and Eqs.(1-2), the theoretical U-
228 values for Cases A and B were calculated, as shown in Table 2.

229

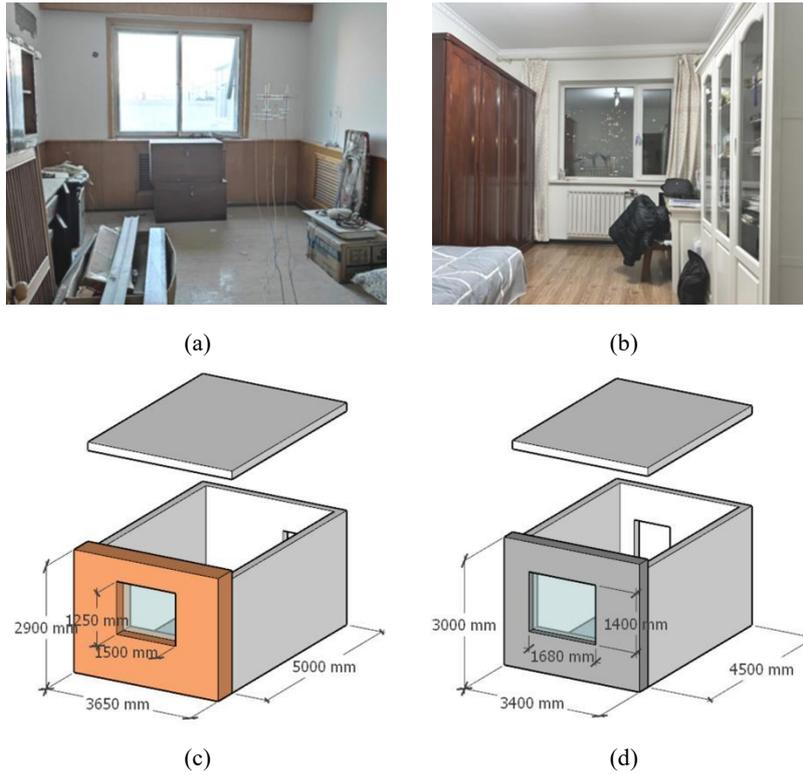


Fig. 3. In-site photos and room dimensions of the test rooms

(a) Photograph of test room A, (b) photograph of test room B, (c) model of test room A, and (d) model of test room B

Table 2. Building material dimensions and thermal properties of Cases A and B

Case	Material	Thickness [mm]	Conductivity [W/(m · K)]	Density [kg/(m ³)]	Specific Heat Capacity [J/(kg · K)]	Layering sketch
A	1 Cement mortar	20	0.93	1800	1050	
	2 EPS insulation	80	0.03	28.5	1650	
	3 Clay brick	240	0.78	1700	840	
	4 Cement mortar	10	0.93	1800	1050	
B	1 Cement mortar	15	0.93	1800	1050	
	2 EPS insulation	100	0.03	28.5	1650	
	3 Reinforced concrete	210	1.75	2500	920	
	4 Cement mortar	10	0.93	1800	1050	

Theoretical U-value: case A: 0.315 W/(m² · K) ; case B: 0.274 W/(m² · K)

2.3. In-situ U-value measurements

2.3.1 Measurement conditions and instrumentation

Due to the huge temperature difference between the winter and summer in the severe cold region, the U-values of the building envelopes may fluctuate differently under different seasonal conditions. In order to comprehensively study the fluctuation of U-values in different seasons, the measurement

243 period included summer, transition season, and winter. As shown in Table 3, the in-situ
 244 measurements were conducted from 17 January 2023 to 1 July 2023. Each tested envelope was
 245 measured six times, including three seasons, and each measurement lasted no less than twelve days
 246 to obtain reliable results according to ISO 9869-1 [38]. The measured dynamic U-values of each
 247 tested envelope included six values, which were the average U-values of the six measurement
 248 periods. To minimise the influence of human factors on the heat flow, no one entered the test rooms,
 249 and the windows and doors were kept closed during the measurement periods. There was no cooling
 250 system in the test rooms and the heating system was always switched off.

251

252 The in-situ U-value measurement system consisted of three parts: (1) two heat flux meters that
 253 generated an electrical signal when heat flowed through the tested envelopes; (2) indoor and outdoor
 254 environment recorders that recorded the temperature and RH every five minutes; and (3) a data
 255 logger for recording the measured heat flow every five minutes. A sketch of the tested envelope with
 256 all instruments is shown in Figure 4 (a), and the placement spots of heat flow sensors on the internal
 257 surfaces of two tested envelopes is shown in Figure 4(b) and 4(c). Photographs and parameters of
 258 the instruments are shown in Figure 5 and Table 4, respectively. Prior to the measurements, the
 259 tested envelopes were examined using an infrared imager to ensure homogeneous heat transfer in
 260 the tested area, as shown in Figure 5(b) and 5(d), respectively. All the instruments were calibrated
 261 by the manufacturer before use. The heat flux meters were installed at 1.5 m height from the floor
 262 to avoid incorrect measurements [67]. To reduce the influence of solar radiation on the U-value
 263 measurements, both tested envelopes were oriented north [38].

264

265 **Table 3. In-situ U-value measurement periods of Cases A and B**

Case No.	Measurement periods	Case No.	Measurement periods
Case A-1	2023.01.16–2023.01.29 (14D)	Case B-1	2023.02.02–2023.02.13 (12D)
Case A-2	2023.02.15–2023.03.01 (15D)	Case B-2	2023.03.03–2023.03.14 (12D)
Case A-3	2023.03.16–2023.03.31 (16D)	Case B-3	2023.04.03–2023.04.14 (12D)
Case A-4	2023.04.16–2023.04.29 (14D)	Case B-4	2023.05.01–2023.05.14 (14D)
Case A-5	2023.05.16–2023.05.31 (16D)	Case B-5	2023.06.02–2023.06.14 (13D)
Case A-6	2023.06.16–2023.07.01 (16D)	Case B-6	2023.07.03–2023.07.15 (13D)

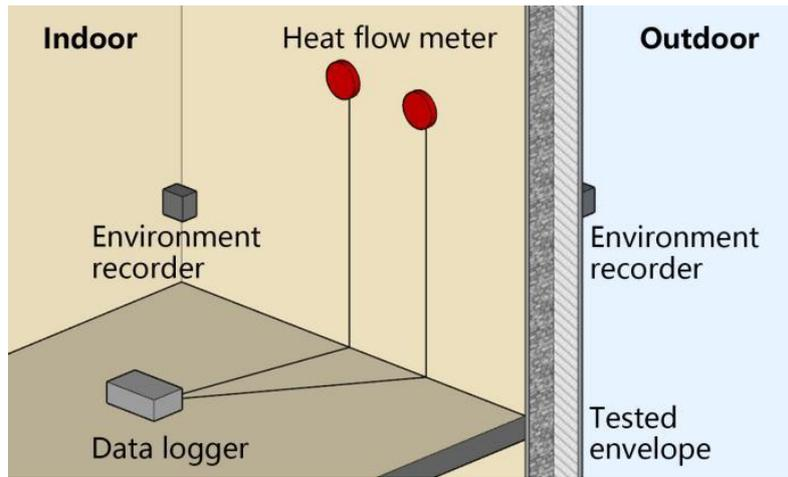
266

267 **Table 4. Parameters of instruments**

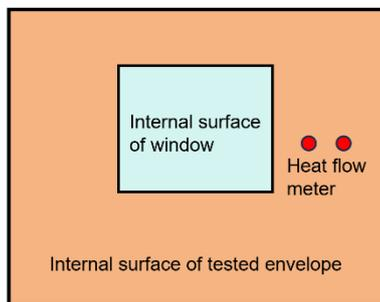
Instrument	Brand	Model	Measuring range	Accuracy	Resolution
Heat flux meter	Hukseflux	HFP01	-2000 to +2000 W/m ²	± 3 %	0.001W/m ²
Indoor and outdoor environment recorders	JDRK	COS-04	T: -40 to +80 °C RH: 0 to +100%	T: ±0.1 °C RH: ±1.5%	T: 0.1 °C RH: 0.1%
Data logger	Yustek	IUDAQ 256-8	NA	NA	NA

268

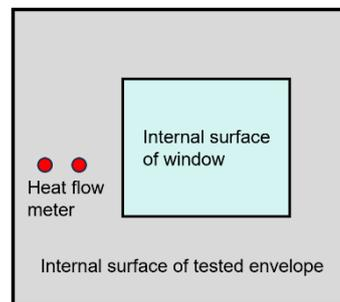
269



(a)



(b)

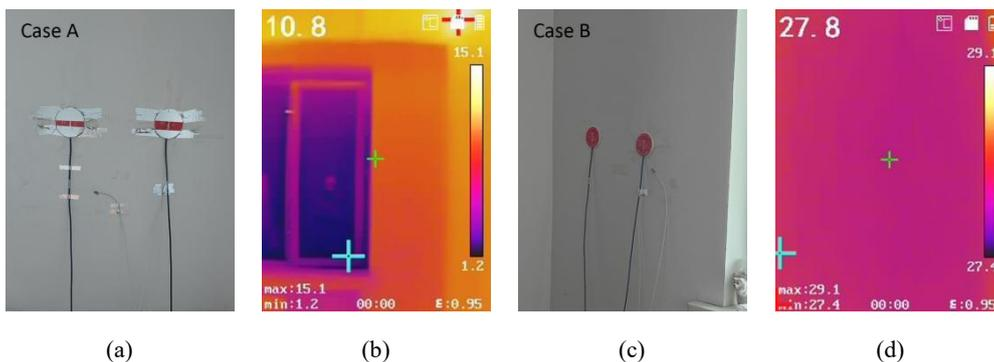


(c)

Fig. 4. Sketches of tested envelopes

(a) The tested envelope with all instruments, (b) the placement of two heat flow sensors on the internal surface of the tested envelope in Case A, (c) the placement of two heat flow sensors on the internal surface of the tested envelope in Case B

270
271
272
273
274
275
276



(a)

(b)

(c)

(d)

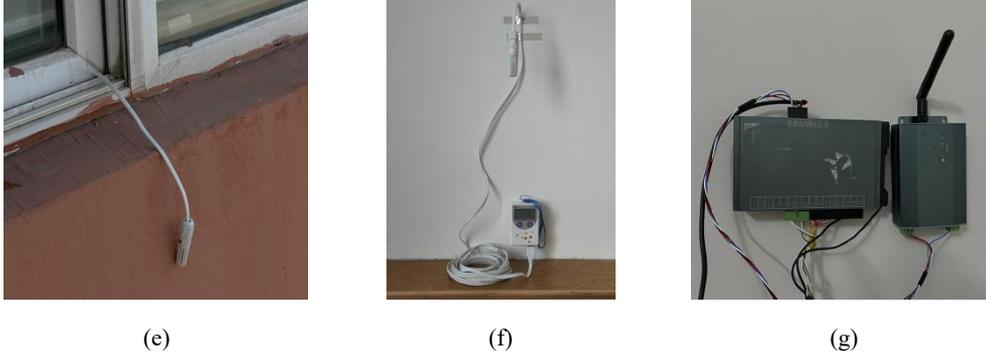


Fig. 5. In-situ measurement photos

(a) Heat flux meters in Case A, (b) infrared image of Case A, (c) heat flux meters in Case B, (d) infrared image of Case B, (e) sensor of the outdoor environment recorder, (f) indoor environment recorder, and (g) set of data loggers

2.2.2 Removing the heat storage effect – heat flow meter (RHS-HFM) method

Because the measurement period included summer, the direction of the indoor and outdoor temperature differences sometimes changed. The changes in the direction of the heat flow were slower than the changes in the direction of the temperature difference owing to the heat storage capacity of the envelopes. This delay in the heat flow can lead to errors according to ISO 9869-1 [38]. To overcome errors caused by unstable temperature differences and heat flow, the removing the heat storage effect - heat flow meter (RHS-HFM) method was proposed by Shi et al. to remove the heat storage effect and overcome seasonal limitations [68] and has been the focus of many researchers [69-71]. According to this method, the average U-values and dynamic U-values consisting of the average U-values of the six measurement periods were calculated using Eqs.(3-6):

$$U = \frac{\overline{q_N}}{\overline{\Delta T_N}} \text{ [W/(m}^2 \cdot \text{K)]} \quad (3)$$

$$\overline{\Delta T_N} = \frac{\sum_{i=1}^n \overline{\Delta T_{\text{period},i}}}{n} \text{ [K]} \quad (4)$$

$$\overline{\Delta T_{\text{period},i}} \approx \frac{|T_{\text{in,max}} - T_{\text{out,max}}| + |T_{\text{in,min}} - T_{\text{out,min}}|}{2} \text{ [K]} \quad (5)$$

$$\overline{q_N} = \frac{\sum_{i=1}^n \overline{|q_{\text{period},i}|}}{n} \text{ [W/m}^2\text{]} \quad (6)$$

The U-value equals the average temperature difference of total measurement duration ($\overline{\Delta T_N}$) divided by the average heat flow density of total measurement duration ($\overline{q_N}$), as formulated in Eq.(3). Compared with outdoor temperature fluctuations, indoor temperature fluctuations are delayed due to the heat storage effects of the envelopes. To remove the effects of heat storage, the calculation of $\overline{\Delta T_N}$ can be approximated and simplified, as shown in Eqs.(4-5). The total measurement duration (N) includes n periods of 24 hours each. $\overline{\Delta T_N}$ is the sum of average temperature difference of each period ($\overline{\Delta T_{\text{period},i}}$) divided by the number of periods, as formulated in Eq.(4). In each period, $\overline{\Delta T_{\text{period},i}}$ approximates the average of two values: (a) the temperature difference between the highest indoor temperature and the highest outdoor temperature and (b) the temperature difference

304 between the lowest indoor temperature and the lowest outdoor temperature, as formulated in Eq.(5).
305 $\overline{q_N}$ is the sum of the average heat flow densities for each period ($\overline{q_{period,i}}$) divided by the number
306 of periods, as shown in Eq.(6).

307

308 2.3. Building energy simulation

309

310 The operational energy based on theoretical, average, and dynamic U-values was obtained through
311 building energy simulations. EnergyPlus was used in this study because it has been widely adopted
312 [69, 72, 73]. The building energy simulations were divided into two groups: Group A (the brick
313 building) and Group B (the RC building). For each group, the reference building was simulated in
314 Harbin by changing the U-values of the envelopes. For simulating building energy of each group
315 based on the dynamic U-values, six simulations were performed to correspond to the six
316 measurement periods. The input U-value was changed for each simulation. The input U-value in the
317 simulation for each measurement period was the measured average U-value per period. Six
318 simulations were also performed to estimate the building energy consumption based on the
319 theoretical or average U-value. The input theoretical or average U-values were kept constant during
320 each simulation.

321

322 Three types of U-values were applied to perform operational energy simulations for a reference
323 building (Figure 6). The reference building is a widely used dwelling in a severe cold region of
324 China. It consists of six floors, each with an area of 520 m². For each group, the simulation time
325 was consistent with the measurement period. Weather files for Harbin were derived from in-situ
326 measurements (T_{out} and RH_{out}) and weather station data during the measurement periods (solar
327 radiation, wind speed, and direction). Because the two tested envelopes were built in different years
328 in China, the major parameters of the building materials in Groups A and B were set according to
329 two versions of the Design Standard for Energy Efficiency of Residential Buildings in Severe Cold
330 and Cold Regions of China (JGJ 26-1986 and JGJ 26-2010) [74, 75], as shown in Table 5.

331

332 To investigate the effect of U-value changes on building energy consumption, all simulations were
333 set to no occupants and no windows or doors were open. Heating and cooling systems only were
334 activated when the indoor temperature was below 20 °C or above 27 °C. To change the U-values of
335 the envelopes without affecting the thermal mass of the envelopes, the envelopes of the reference
336 building were set by changing the airgap thermal resistance to match the measured U-values in
337 operational energy simulation [16]. Meanwhile, other parameters related to building materials were
338 not changed.

339

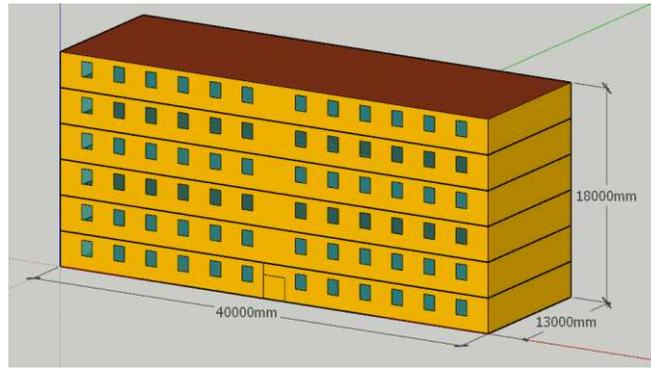


Fig. 6. Reference building model

340
341
342
343

Table 5. Major parameters of reference buildings in Group A and Group B

	Group A	Group B
Building envelope type	Brick envelope	RC envelope
Design standard	JGJ 26-1986	JGJ 26-2010
U-values of roof [W/(m ² · K)]	0.2	0.2
U-values of floors [W/(m ² · K)]	0.50	0.43
U-values of windows [W/(m ² · K)]	1.85	1.55
G-value of windows	0.55	0.39
Infiltration ACH [h ⁻¹]	0.51	0.50

344
345
346

3 Results

347
348

3.1. Measured U-values of test envelopes

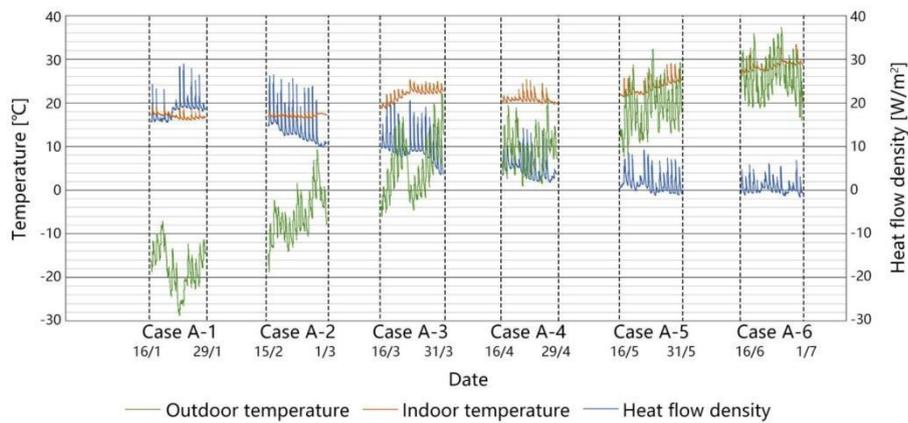
349
350
351
352
353
354
355
356
357
358
359
360
361
362
363
364
365
366
367

The indoor and outdoor temperatures and heat flow density in Cases A and B were recorded, and the measurement data are presented in Figures 7-8. During the measurement period (16/01/2023-15/07/2023), the outdoor temperature in Harbin varied significantly, with a minimum temperature of -28.7 °C in winter and a maximum temperature of 36.8 °C in summer. The indoor temperature in Case A varied from 16.0 °C to 32.4 °C. The indoor temperature in Case B varied less, ranging from 19.7 °C to 28.8 °C. The indoor temperature in Cases A and B was approximately 20 °C in winter. Although the heating system was switched off in the test rooms, the neighbouring rooms contained heating systems that influenced the indoor environment. In Case A, the heat flow density was always positive in winter and early spring (Cases A-1 to A-4), indicating that the direction of the heat flow density did not change. In contrast, in late spring and summer (Cases A-5 and A-6), the heat flow density was sometimes negative, indicating a change in the direction of the heat flow. This is because the outdoor temperature is not always higher than the indoor temperature during late spring and summer in severe cold regions, and the direction of the temperature difference changed, resulting in a change in the direction of the heat flow. This phenomenon was also observed in Case B-6. Owing to the thermal storage of the envelopes, there was a delay in heat transfer, and the change in the direction of the temperature difference preceded the change in the direction of the heat flow density. If the heat transfer delay is not processed, the calculated U-value appears negative when the temperature difference is opposite the direction of the heat flow density, which leads to an error. Therefore, to reduce the effect of a delay in heat transfer, the RHS-HFM method was chosen to

368 calculate the U-values of the envelopes.

369

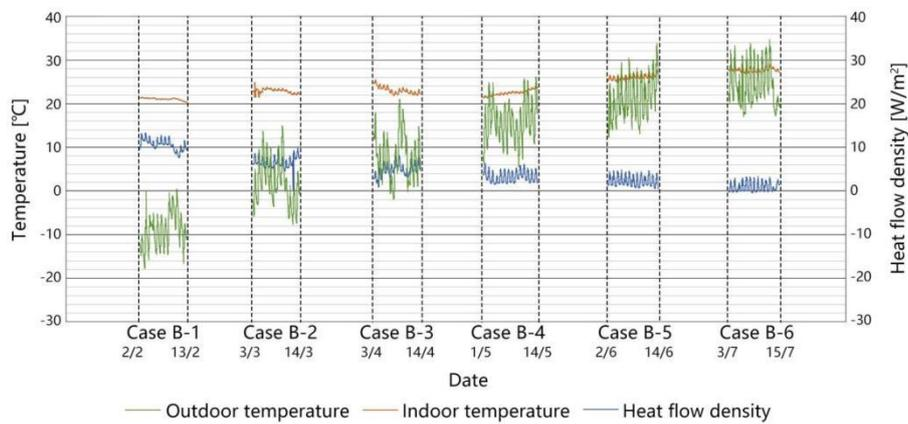
370 As depicted in Figure 9, the measured U-values included dynamic and average U-values. The
371 dynamic U-values in Case A included six values that were the average U-values for Cases A-1 to A-
372 6. Meanwhile, the dynamic U-values in Case B included six values, which were the average U-
373 values of Cases B-1 to B-6. The average U-value in each case was calculated based on the data for
374 all the measurement periods. The average U-values exceed the theoretical U-values by 37.8% and
375 22.3% for Cases A and B, respectively. The dynamic U-values of Cases A and B displayed
376 decreasing trends from winter to summer, which were more remarkable in Case A. For both Cases
377 A and B, the U-values in winter exceeded those in summer by 159.8% and 30.8%, respectively. This
378 indicates that the decrease in U-values from winter to summer was not negligible, especially for
379 brick buildings built several decades ago.



380

381

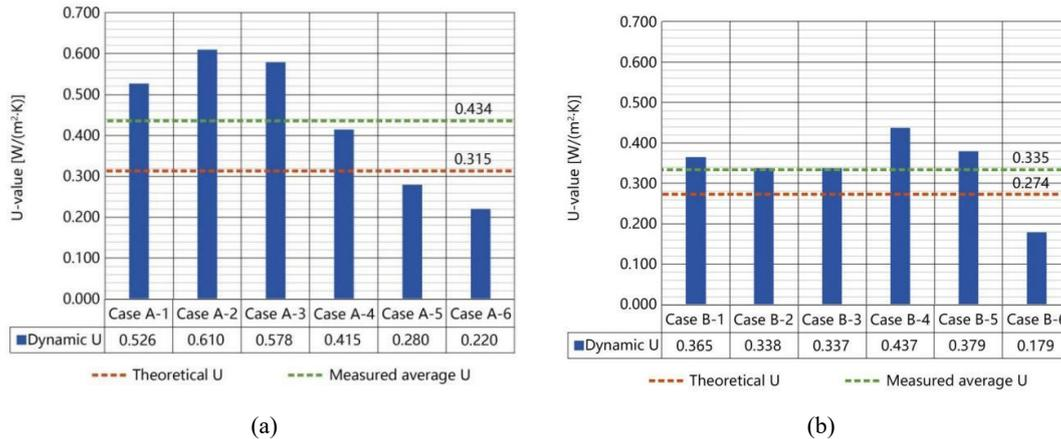
Fig. 7. Measured indoor and outdoor temperature and heat flow density in Case A



382

383

Fig. 8. Measured indoor and outdoor temperature and heat flow density in Case B



(a) (b)
Fig. 9. Theoretical and measured U-values in Cases A and B

(a) dynamic U-values for Case A; (b) dynamic U-values for Case B

384

385

386

387 *3.2. Influence of dynamic U-values on operational energy efficiency in different buildings*

388

389 The theoretical U-values, measured average U-values, and dynamic U-values of Cases A and B were
 390 applied to the building energy simulation of the reference building. The building energy simulations
 391 were divided into two groups: Groups A and B. Group A included six simulations, named Groups
 392 A-1 to A-6. The simulation times of the six simulations were based on the measurement periods in
 393 Case A (cases A-1 to A-6). Group B also included six simulations, named Groups B-1 to B-6; hence,
 394 the simulation times of the six simulations were based on the measurement periods in Case B (Cases
 395 B-1 to B-6). In all simulations, when the indoor temperature exceeded 20–27 °C, the heating or
 396 cooling system was switched on.

397

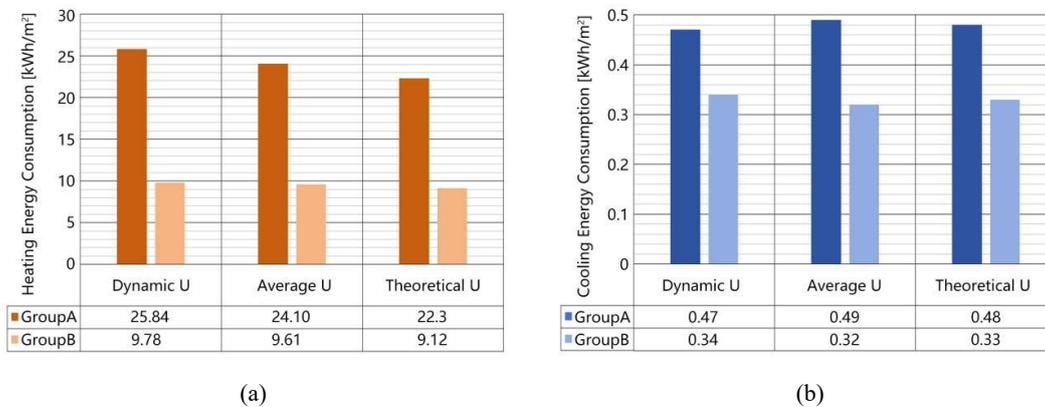
398 The heating and cooling energy consumption based on the theoretical, average, and dynamic U-
 399 values in Groups A and B are presented in Figure 10. Figures 10 (a) and (b) show that the heating
 400 energy consumption is much more than the cooling energy consumption in Groups A and B. For
 401 example, heating energy consumption accounted for 98.2 % and 97.5 % of the total energy
 402 consumption in Groups A and B in the building energy consumption based on dynamic U-value,
 403 respectively. This result was related to the climatic region. In severe cold regions, heating energy is
 404 the major component of energy consumption, accounting for one-third of the total energy use [23].

405

406 As shown in Figure 10 (a), the heating energy consumption in Group A was 16.06 kWh/m², 14.49
 407 kWh/m², and 13.18 kWh/m² more than that in Group B according to building energy simulation
 408 results based on the dynamic, average, and theoretical U-values, respectively. It suggested that the
 409 more aged brick envelope had worse insulation properties compared to the RC envelope. Compared
 410 with the measured average U-values, the measured dynamic U-values exerted a more significant
 411 effect on heating energy. The influence of the measured dynamic U-values on heating energy
 412 consumption was more significant in Group A than in Group B. Figure 10 (a) shows that the heating
 413 energy based on the measured dynamic U-values exceeded that based on the theoretical U-values
 414 by 15.9% and 7.2% in Groups A and B, respectively. The heating energy based on the measured
 415 average U-values exceeded that based on the theoretical U-values by 8.1% and 5.4% for Groups A
 416 and B, respectively.

417

418 However, the differences of the cooling energy consumption between Groups A and B were not as
 419 significant as that of the heating energy consumption between Groups A and B. As shown in Figure
 420 10 (b), the cooling energy consumption in Group A was more than 0.13 kWh/m², 0.17 kWh/m²,
 421 and 0.15 kWh/m² more than in Group B according to building energy simulation results based on
 422 the dynamic, average, and theoretical U-values, respectively. In Groups A and B, the measured
 423 average and dynamic U-values showed insignificant differences in cooling energy consumption.
 424 The cooling energy based on the measured dynamic U-values was less than that based on the
 425 theoretical U-values by 2.1% in Group A. The cooling energy based on the measured dynamic U-
 426 values exceeded that based on the theoretical U-values by 3.0% in Group B. The cooling energy
 427 based on the measured average U-values exceeded that based on the theoretical U-values by 2.1%
 428 in Group A. The cooling energy based on the measured average U-values was less than that based
 429 on the theoretical U-values by 3.0 % in Group B.
 430



431 **Fig.10.** Operational energy simulation results for the reference building in both Group A and Group B based on
 432 different U-values

433 (a) Heating energy simulation results; (b) cooling energy simulation results

434

435 *3.3. Influence of dynamic U-values on operational energy efficiency in different seasons*

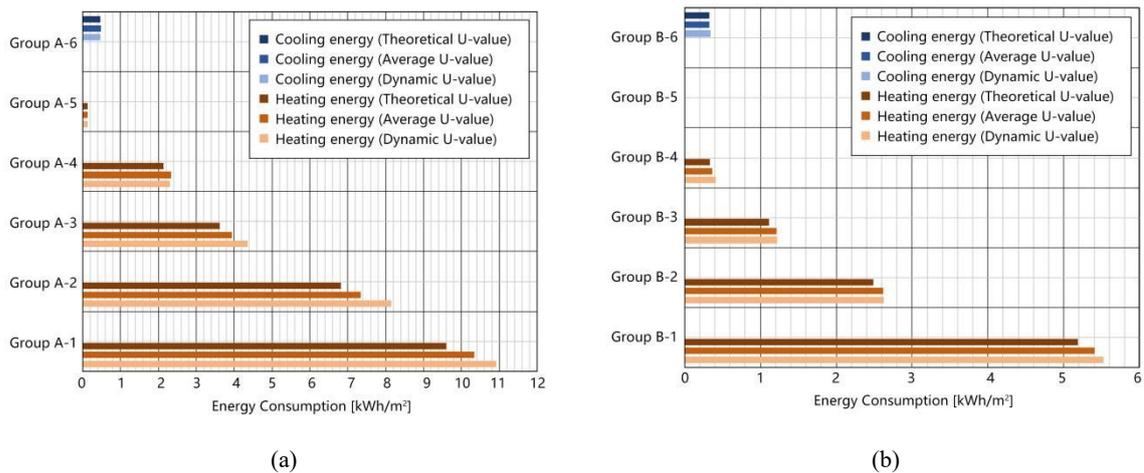
436

437 The heating and cooling energy consumption for each period is presented in Figure 11. The energy
 438 consumption based on the three types of U-values exhibited different characteristics during different
 439 seasons. The heating energy consumption in winter (including Groups A-1, A-2, and B-1) was
 440 higher than that in the transition season (including Groups A-3, A-4, A-5, B-2, B-3, and B-4). The
 441 gaps between the heating energy consumption based on the three types of U-values were more
 442 noticeable in winter than in the transition season. For example, in winter, the heating energy based
 443 on measured dynamic U-values exceeded that based on the theoretical U-values by 1.31 and 0.34
 444 kWh/m² in Groups A-1 and B-1, respectively. The heating energy based on measured dynamic U-
 445 values exceeded that based on measured average U-values by 0.58 and 0.11 kWh/m² in Groups
 446 A-1 and B-1, respectively. In the transition season, the heating energy based on measured dynamic
 447 U-values exceeded that based on the theoretical U-values by 0.17 kWh/m² and 0.07 kWh/m²
 448 in Groups A-4 and B-4. The heating energy based on measured dynamic U-values was less than that
 449 based on measured average U-values by 0.03 kWh/m² in Group A-4 and more than that based on
 450 measured average U-values 0.05 kWh/m² in Group B-4.

451

452 The gaps between the cooling energy consumptions based on the three types of U-values were
453 unremarkable in summer (including Groups A-6, B-5, and B-6). The cooling energy based on
454 measured dynamic U-values was less than that based on the theoretical U-values by 0.01 kWh/m²
455 in Group A-6 and more than that based on the theoretical U-values by 0.01 kWh/m² in Group B-
456 6. The cooling energy based on measured dynamic U-values was less than that based on measured
457 average U-values by 0.02 kWh/m² in Group A-6 and more than that based on measured average
458 U-values 0.02 kWh/m² in Group B-6.

459



460 **Fig. 11.** Detailed information on heating and cooling energy simulation results for both Group A (from A-1 to A-6)
461 and Group B (from B-1 to B-6)

462 (a) Detailed simulation results for Group A and (b) detailed simulation results for Group B

463

464 4 Discussion

465

466 The decrease in U-values observed from winter to summer is a prominent phenomenon. During
467 winter in severe cold regions, the porous materials containing moisture in the building envelopes
468 are frozen and gradually thawed in the summer. According to existing studies, the thermal
469 conductivity of pure ice is approximately 2.22 W/(m · K) at -10 °C, whereas that of water is 0.60
470 W/(m · K) at 20 °C [76]. The change in the physical state of the moisture within the envelopes
471 from freezing to thawing may contribute to a decrease in the thermal conductivity of porous building
472 materials. The U-values of the envelopes also decreased as they were proportional to the thermal
473 conductivity of the building materials. Several researchers have reported similar findings for
474 moisture-containing porous materials. For instance, Chuvilin et al. found that frozen porous
475 sediments with high moisture contents had higher thermal conductivities than the unfrozen
476 sediments [77]. Tang et al. revealed that the thermal conductivity of frozen soil-rock mixture
477 decreased by 30.18% from -10 to 0 °C because of water-ice transition [78]. Vu et al. focused on the
478 thermal conductivity of sandy soils in different states and revealed that the thermal conductivity of
479 frozen sandy soils was considerably higher than that of unfrozen sandy soils during the
480 freeze-thaw process [79].

481

482 The decreasing trend in the U-values of the tested brick envelope was more significant than those

483 of the tested RC buildings and the tested brick envelope had higher U-values in winter. The tested
 484 brick envelope has been built decades before the tested RC envelope, and it may have had a higher
 485 moisture content. There may be various reasons for the higher moisture content in the older brick
 486 envelope. For example, the deterioration of the building materials or technical weaknesses in the
 487 construction process may lead to an increased infiltration rate through the older brick envelope,
 488 thereby leading to a higher moisture content [66, 80, 81]. These findings illustrate the importance
 489 of moisture barriers in envelopes, especially old envelopes, to mitigate excessive heat loss during
 490 the heating-intensive season. Many buildings were built several decades ago in the severe cold
 491 regions of China. The insulation performance of these buildings does not meet contemporary
 492 building standard requirements [82, 83]. One of the practical retrofit options could be adding a
 493 moisture barrier to the external surface of envelopes to reduce heating energy use in winter.

494
 495 Some cities in various countries have similar energy requirements with Harbin. The HDD18 and
 496 CDD26 of several typical cities are shown in Table 6, and data were derived from weather station
 497 data [84]. In-situ U-value measurements over the long term can contribute to improving heating
 498 energy consumption simulations in these cities. The inputs of both the measured dynamic and
 499 average U-values can influence the heating energy simulation. When simulating the long-term
 500 operational energy in a severe cold region, inputting the measured dynamic U-values could have a
 501 more significant impact on the heating energy simulation results of order brick buildings than those
 502 of newer RC buildings. However, the input of the measured U-values does not significantly affect
 503 the cooling energy simulation results. This may be associated with a relatively low proportion of
 504 cooling energy consumption in severe cold regions [85].

505
 506

Table 6. The HDD18 and CDD26 of several typical cities

City	HDD18 [°C · d]	CDD26 [°C · d]
Harbin	5032	14
Oslo	4431	2
Helsinki	4312	8
Edinburgh	3138	1
Stockholm	3762	5
Reykjavik	4586	0

507

508 This study had three limitations: (1) only the northern envelopes were chosen for measurement to
 509 minimise the effects of solar radiation on the accuracy of the measurements. The dynamic U-values
 510 of the other oriented envelopes may have different characteristics, which require systematic and
 511 detailed research in the future. (2) In-situ measurements were conducted on only two envelopes for
 512 several months. In future studies, more envelopes with different orientations should be measured
 513 throughout the year to obtain more comprehensive data. The tested envelopes included not only
 514 conventional envelopes but also bio-based envelopes, such as cross-laminated timber envelopes. (3)
 515 The building parameters that affect U-values were not measured, such as infiltration rates of tested
 516 envelopes. In future studies, the infiltration rates of different envelopes can be measured, and the
 517 quantitative relationship between the dynamic U-values and the infiltration rates can be discussed.
 518 This relationship can explain the process that generates dynamic U-values more clearly. It can
 519 inform building maintenance, especially retrofitting of old buildings.

520

521 **5 Conclusion**

522

523 In-situ U-value measurements of two typical building envelopes in Harbin were conducted from
524 winter to summer in 2023. The measured average and dynamic U-values of the brick and RC
525 envelopes were obtained. To study the influence of dynamic U-values on building energy efficiency,
526 the building energy simulation results based on the theoretical U-values, measured average U-values,
527 and dynamic U-values of the tested brick and RC envelopes were compared. The main conclusions
528 of this study are as follows.

529

- 530 (1) The fluctuations in U-values of typical building envelopes were substantial in severe cold
531 regions. In the dynamic U-values of both brick and RC envelopes, the higher U-values were
532 observed in winter months. The more aged brick envelopes displayed more significant U-value
533 fluctuations than the RC envelopes. The higher U-values of typical building envelopes in
534 winter may be attributed to the higher moisture content, illustrating the importance of moisture
535 barriers in envelopes. In the severe cold regions of China, adding a moisture barrier should
536 become an important retrofitting solution to reduce heating energy consumption in winter.
- 537 (2) The effect of dynamic U-values on the heating energy consumption of the reference brick
538 building was greater than that of the reference RC building in severe cold regions. This
539 indicates that inputting dynamic U-values can have a more significant impact on the heating
540 energy simulation results of brick buildings built several decades ago than on those of newer
541 RC buildings.
- 542 (3) The impact of dynamic U-values on operational energy consumption depends on the season in
543 severe cold regions. The heating energy consumption based on dynamic U-values exceeded
544 that based on theoretical U-values by 15.9% and 7.2% in the reference brick and RC buildings,
545 respectively. Conversely, the differences between the cooling energy simulation results based
546 on different types of U-values were not significant. This indicates that long-term dynamic U-
547 value measurements could contribute to improving heating energy consumption simulations in
548 severe cold regions.

549

550 This study contributes to minimising the gap between building energy simulations and actual energy
551 consumption. Reliable measured data can be used to optimise building performance simulations and
552 manage energy use more efficiently and accurately. This paper builds a foundation for further study
553 on the dynamic U-values of different types of envelopes, including inorganic material envelopes
554 and bio-based envelopes, in various climate regions. This dataset of dynamic U-values will provide
555 more comprehensive and reliable references for building thermal attributes in building energy
556 simulation.

557

558 **Funding**

559 This research is supported by Key Research and Development Program Project of Heilongjiang
560 Province, China in 2023 (Innovation Base, JD2023SJ01).

561

562 **Data availability**

563 Data will be made available on request.

564

565 References

- 566 1. Reveshti, A.M., A. Ebrahimpour, and J. Razmara, *Investigating the effect of new and old*
567 *weather data on the energy consumption of buildings affected by global warming in different*
568 *climates*. International Journal of Thermofluids, 2023. **19**: p. 100377.
- 569 2. Cao, X., X. Dai, and J. Liu, *Building energy-consumption status worldwide and the state-of-the-*
570 *art technologies for zero-energy buildings during the past decade*. Energy and Buildings, 2016.
571 **128**: p. 198-213.
- 572 3. Guo, S., et al., *Global comparison of building energy use data within the context of climate*
573 *change*. Energy and Buildings, 2020. **226**: p. 110362.
- 574 4. Li, H., et al., *Integrated building envelope performance evaluation method towards nearly zero*
575 *energy buildings based on operation data*. Energy and Buildings, 2022. **268**: p. 112219.
- 576 5. Guo, Y.-Y., *Revisiting the building energy consumption in China: Insights from a large-scale*
577 *national survey*. Energy for Sustainable Development, 2022. **68**: p. 76-93.
- 578 6. Chang, C., et al., *Data and analytics for heating energy consumption of residential buildings:*
579 *The case of a severe cold climate region of China*. Energy and Buildings, 2018. **172**: p. 104-115.
- 580 7. Housing, M.o. and U.-R.D.o.t.P.s.R.o. China, *Code for Thermal Design of Civil Building (GB*
581 *50176-2016)*. 2016, China Architecture & Building Press Beijing, China.
- 582 8. Leng, H., et al., *Urban morphology and building heating energy consumption: Evidence from*
583 *Harbin, a severe cold region city*. Energy and Buildings, 2020. **224**: p. 110143.
- 584 9. Nematchoua, M.K., et al., *Analysis of environmental impacts and costs of a residential building*
585 *over its entire life cycle to achieve nearly zero energy and low emission objectives*. Journal of
586 Cleaner Production, 2022. **373**: p. 133834.
- 587 10. Wang, P., et al., *Positivity and difference of influence of built environment around urban park*
588 *on building energy consumption*. Sustainable Cities and Society, 2023. **89**: p. 104321.
- 589 11. Ni, S., et al., *Research on indoor thermal comfort and energy consumption of zero energy*
590 *wooden structure buildings in severe cold zone*. Journal of Building Engineering, 2023. **67**: p.
591 105965.
- 592 12. Dougherty, T.R. and R.K. Jain, *Invisible walls: Exploration of microclimate effects on building*
593 *energy consumption in New York City*. Sustainable Cities and Society, 2023. **90**: p. 104364.
- 594 13. Xu, H., et al., *LOD2 for energy simulation (LOD2ES) for CityGML: A novel level of details model*
595 *for IFC-based building features extraction and energy simulation*. Journal of Building
596 Engineering, 2023. **78**: p. 107715.
- 597 14. Choi, K., et al., *Review of infiltration and airflow models in building energy simulations for*
598 *providing guidelines to building energy modelers*. Renewable and Sustainable Energy Reviews,
599 2023. **181**: p. 113327.
- 600 15. Klemp, S., A. Abida, and P. Richter, *A method and analysis of predicting building material U-*
601 *value ranges through geometrical pattern clustering*. Journal of Building Engineering, 2021. **44**:
602 p. 103243.
- 603 16. Bruno, R. and P. Bevilacqua, *Heat and mass transfer for the U-value assessment of opaque walls*
604 *in the Mediterranean climate: Energy implications*. Energy, 2022. **261**: p. 124894.
- 605 17. Ficco, G., et al., *U-value in situ measurement for energy diagnosis of existing buildings*. Energy
606 and Buildings, 2015. **104**: p. 108-121.

- 607 18. Ahern, C., B. Norton, and B. Enright, *The statistical relevance and effect of assuming pessimistic*
608 *default overall thermal transmittance coefficients on dwelling energy performance certification*
609 *quality in Ireland*. Energy and Buildings, 2016. **127**: p. 268-278.
- 610 19. Albatici, R., A.M. Tonelli, and M. Chiogna, *A comprehensive experimental approach for the*
611 *validation of quantitative infrared thermography in the evaluation of building thermal*
612 *transmittance*. Applied Energy, 2015. **141**: p. 218-228.
- 613 20. Fernandes, M.S., et al., *The impact of thermal transmittance variation on building design in the*
614 *Mediterranean region*. Applied Energy, 2019. **239**: p. 581-597.
- 615 21. Ihara, T., A. Gustavsen, and B.P. Jelle, *Effect of facade components on energy efficiency in office*
616 *buildings*. Applied Energy, 2015. **158**: p. 422-432.
- 617 22. Guo, H., et al., *A Comparison of the Energy Saving and Carbon Reduction Performance between*
618 *Reinforced Concrete and Cross-Laminated Timber Structures in Residential Buildings in the*
619 *Severe Cold Region of China*. Sustainability, 2017. **9**(8).
- 620 23. Dong, Y., et al. *Assessment of Energy Saving Potential by Replacing Conventional Materials by*
621 *Cross Laminated Timber (CLT)—A Case Study of Office Buildings in China*. Applied Sciences,
622 2019. **9**, DOI: 10.3390/app9050858.
- 623 24. Kotsiris, G., et al., *Dynamic U-value estimation and energy simulation for green roofs*. Energy
624 and Buildings, 2012. **45**: p. 240-249.
- 625 25. Yu, J., W.-S. Chang, and Y. Dong *Building Energy Prediction Models and Related Uncertainties:*
626 *A Review*. Buildings, 2022. **12**, DOI: 10.3390/buildings12081284.
- 627 26. (ISO), I.O.f.S., *ISO 6946, Building components and building elements – Thermal resistance and*
628 *thermal transmittance – Calculation method*. 2007.
- 629 27. O'Hegarty, R., et al., *In-situ U-value monitoring of highly insulated building envelopes: Review*
630 *and experimental investigation*. Energy and Buildings, 2021. **252**: p. 111447.
- 631 28. Wang, Y., et al., *Experimental investigation on thermal conductivity of aerogel-incorporated*
632 *concrete under various hygrothermal environment*. Energy, 2019. **188**: p. 115999.
- 633 29. Asdrubali, F., et al., *Evaluating in situ thermal transmittance of green buildings masonries—A*
634 *case study*. Case Studies in Construction Materials, 2014. **1**: p. 53-59.
- 635 30. Gumbarević, S., et al. *Combining Deep Learning and the Heat Flux Method for In-Situ Thermal-*
636 *Transmittance Measurement Improvement*. Energies, 2022. **15**, DOI: 10.3390/en15145029.
- 637 31. Evangelisti, L., et al., *A methodological approach for heat-flow meter data post-processing*
638 *under different climatic conditions and wall orientations*. Energy and Buildings, 2020. **223**: p.
639 110216.
- 640 32. Gaspar, K., M. Casals, and M. Gangoellis, *In situ measurement of façades with a low U-value:*
641 *Avoiding deviations*. Energy and Buildings, 2018. **170**: p. 61-73.
- 642 33. Meng, X., et al., *Feasibility experiment on the simple hot box-heat flow meter method and the*
643 *optimization based on simulation reproduction*. Applied Thermal Engineering, 2015. **83**: p. 48-
644 56.
- 645 34. Bienvenido-Huertas, D., et al. *Determining the U-Value of Façades Using the Thermometric*
646 *Method: Potentials and Limitations*. Energies, 2018. **11**, DOI: 10.3390/en11020360.
- 647 35. ISO, *ISO 9869-2, Thermal insulation — Building elements — In-situ measurement of thermal*
648 *resistance and thermal transmittance — Part 2: Infrared method for frame structure dwelling*.
649 2018.

- 650 36. ASTM, *ASTM C1060, Standard Practice for Thermographic Inspection of Insulation Installations*
651 *in Envelope Cavities of Frame Buildings*. 2011.
- 652 37. Ahmad, A., M. Maslehuddin, and L.M. Al-Hadhrami, *In situ measurement of thermal*
653 *transmittance and thermal resistance of hollow reinforced precast concrete walls*. Energy and
654 Buildings, 2014. **84**: p. 132-141.
- 655 38. ISO, *ISO 9869-1, Thermal Insulation, Building Elements, In-Situ Measurement of Thermal*
656 *Resistance and Thermal Transmittance-Part 1: Heat Flow Meter Method*. 2014.
- 657 39. ASTM, *ASTM C1155-95 Standard, Standard Practice for Determining Thermal Resistance of*
658 *Building Envelope Components from the In-situ Data*. 2007.
- 659 40. Mandilaras, I., et al., *Thermal performance of a building envelope incorporating ETICS with*
660 *vacuum insulation panels and EPS*. Energy and Buildings, 2014. **85**: p. 654-665.
- 661 41. Evangelisti, L., et al. *In Situ Thermal Transmittance Measurements for Investigating Differences*
662 *between Wall Models and Actual Building Performance*. Sustainability, 2015. **7**, 10388-10398
663 DOI: 10.3390/su70810388.
- 664 42. Gaspar, K., M. Casals, and M. Gangoellis, *A comparison of standardized calculation methods for*
665 *in situ measurements of façades U-value*. Energy and Buildings, 2016. **130**: p. 592-599.
- 666 43. Evangelisti, L., et al., *Experimental investigation of the influence of convective and radiative*
667 *heat transfers on thermal transmittance measurements*. International Communications in Heat
668 and Mass Transfer, 2016. **78**: p. 214-223.
- 669 44. Samardzioska, T. and R. Apostolska *Measurement of Heat-Flux of New Type Façade Walls*.
670 Sustainability, 2016. **8**, DOI: 10.3390/su8101031.
- 671 45. Choi, D.S. and M.J. Ko *Comparison of Various Analysis Methods Based on Heat Flowmeters and*
672 *Infrared Thermography Measurements for the Evaluation of the In Situ Thermal Transmittance*
673 *of Opaque Exterior Walls*. Energies, 2017. **10**, DOI: 10.3390/en10071019.
- 674 46. Campbell, N., et al., *Monitoring the hygrothermal and ventilation performance of retrofitted*
675 *clay brick solid wall houses with internal insulation: Two UK case studies*. Case Studies in
676 Construction Materials, 2017. **7**: p. 163-179.
- 677 47. Lelievre, D., T. Colinart, and P. Glouannec, *Hygrothermal behavior of bio-based building*
678 *materials including hysteresis effects: Experimental and numerical analyses*. Energy and
679 Buildings, 2014. **84**: p. 617-627.
- 680 48. Wu, D., et al., *Dynamic hygrothermal behavior and energy performance analysis of a novel*
681 *multilayer building envelope based on PCM and hemp concrete*. Construction and Building
682 Materials, 2022. **341**: p. 127739.
- 683 49. Bennai, F., et al., *Assessment of hygrothermal performance of hemp concrete compared to*
684 *conventional building materials at overall building scale*. Construction and Building Materials,
685 2022. **316**: p. 126007.
- 686 50. Islahuddin, M. and H. Janssen, *Hygric property estimation of porous building materials with*
687 *multiscale pore structures*. Energy Procedia, 2017. **132**: p. 273-278.
- 688 51. Dong, W., et al., *A validation of dynamic hygrothermal model with coupled heat and moisture*
689 *transfer in porous building materials and envelopes*. Journal of Building Engineering, 2020. **32**:
690 p. 101484.
- 691 52. Wang, Y., et al., *Experimental study on the influence of temperature and humidity on the*
692 *thermal conductivity of building insulation materials*. Energy and Built Environment, 2022.

- 693 53. Wang, Y., et al., *The impact of temperature and relative humidity dependent thermal*
694 *conductivity of insulation materials on heat transfer through the building envelope.* Journal of
695 Building Engineering, 2022. **46**: p. 103700.
- 696 54. Wang, Y., et al., *The effect of moisture transfer on the inner surface thermal performance and*
697 *the thermal transmittance of the roof-wall corner building node in high-temperature and high-*
698 *humidity areas.* Journal of Building Engineering, 2021. **44**: p. 102949.
- 699 55. Yang, X.e., et al., *Energy-saving potential prediction models for large-scale building: A state-of-*
700 *the-art review.* Renewable and Sustainable Energy Reviews, 2022. **156**: p. 111992.
- 701 56. Franceschini, P.B. and L.O. Neves, *A critical review on occupant behaviour modelling for*
702 *building performance simulation of naturally ventilated school buildings and potential changes*
703 *due to the COVID-19 pandemic.* Energy and Buildings, 2022. **258**: p. 111831.
- 704 57. Chen, Y., et al., *Physical energy and data-driven models in building energy prediction: A review.*
705 Energy Reports, 2022. **8**: p. 2656-2671.
- 706 58. Zou, Y., et al., *A simulation-based method to predict the life cycle energy performance of*
707 *residential buildings in different climate zones of China.* Building and Environment, 2021. **193**:
708 p. 107663.
- 709 59. Wan, K.K.W., et al., *Impact of climate change on building energy use in different climate zones*
710 *and mitigation and adaptation implications.* Applied Energy, 2012. **97**: p. 274-282.
- 711 60. Krstić, H., et al. *Thermal Performance Assessment of a Wall Made of Lightweight Concrete*
712 *Blocks with Recycled Brick and Ground Polystyrene.* Buildings, 2021. **11**, DOI:
713 10.3390/buildings11120584.
- 714 61. Ratnieks, J., A. Jakovics, and S. Gendelis, *Wall assemblies U-value calculation in test buildings*
715 *using constant power heating.* Energy Procedia, 2018. **147**: p. 207-213.
- 716 62. Lucchi, E., *Thermal transmittance of historical brick masonries: A comparison among standard*
717 *data, analytical calculation procedures, and in situ heat flow meter measurements.* Energy and
718 Buildings, 2017. **134**: p. 171-184.
- 719 63. Peel, M.C., et al., *Updated world map of the Köppen-Geiger climate classification.* 2007. **11**(5):
720 p. 1633-1644.
- 721 64. Statistics, H.B.o., *Seventh National Population Census.* 2020:
722 https://www.harbin.gov.cn/haerbin/c104569/202105/c01_70396.shtml.
- 723 65. (NDRC), P.N.D.a.R.C., *Twelfth Five-Year Plan Guidance on Wall Materials Innovation*
724 <https://zfxgk.ndrc.gov.cn/web/iteminfo.jsp?id=19709>, 2011.
- 725 66. Byun, J., et al., *Proposal of a correction factor for predicting the thermal transmittance of*
726 *building envelopes in existing buildings accounting for aging and environmental conditions.*
727 Building and Environment, 2023. **243**: p. 110658.
- 728 67. Bienvenido-Huertas, D., et al., *Review of in situ methods for assessing the thermal*
729 *transmittance of walls.* Renewable and Sustainable Energy Reviews, 2019. **102**: p. 356-371.
- 730 68. Shi, X., et al., *Investigation of a new kind of in-situ measurement method of thermal resistance*
731 *of building envelope.* Energy and Buildings, 2022. **258**: p. 111803.
- 732 69. Bastos Porsani, G., et al., *Empirical evaluation of EnergyPlus infiltration model for a case study*
733 *in a high-rise residential building.* Energy and Buildings, 2023. **296**: p. 113322.
- 734 70. Chen, L., et al., *A new method for measuring thermal resistance of building walls and analyses*
735 *of influencing factors.* Construction and Building Materials, 2023. **385**: p. 131438.

- 736 71. Xing, L., et al., *A thermal balance method for measuring thermal conductivity by compensation*
737 *of electric cooling or heating based on thermoelectric modules*. International Journal of
738 Thermal Sciences, 2023. **189**: p. 108264.
- 739 72. Chen, Y., T. Hong, and M.A. Piette, *Automatic generation and simulation of urban building*
740 *energy models based on city datasets for city-scale building retrofit analysis*. Applied Energy,
741 2017. **205**: p. 323-335.
- 742 73. Deshko, V., et al., *Evaluation of energy use for heating in residential building under the influence*
743 *of air exchange modes*. Journal of Building Engineering, 2021. **42**: p. 103020.
- 744 74. JGJ26-1986, *Standard for energy conservation design of new heating residential buildings 民用*
745 *建筑节能设计标准(采暖居住建筑部分)*. 1986.
- 746 75. JGJ26-2010, *Design Standard for Energy Efficiency of Residential Buildings in Severe Cold and*
747 *Cold Zones 严寒和寒冷地区居住建筑节能设计标准*. 2010.
- 748 76. Guo, S., et al., *Effective thermal conductivity of reservoir freshwater ice with attention to high*
749 *temperature*. Annals of Glaciology, 2013. **54**(62): p. 189-195.
- 750 77. Evgeny, C., et al., *Effect of Ice and Hydrate Formation on Thermal Conductivity of Sediments*, in
751 *Impact of Thermal Conductivity on Energy Technologies*, S. Aamir, Editor. 2018, IntechOpen:
752 Rijeka. p. Ch. 7.
- 753 78. Tang, L., et al., *Thermal conductivity changing mechanism of frozen soil-rock mixture and a*
754 *prediction model*. International Journal of Heat and Mass Transfer, 2023. **216**: p. 124529.
- 755 79. Vu, Q.H., J.-M. Pereira, and A.M. Tang, *Effect of clay content on the thermal conductivity of*
756 *unfrozen and frozen sandy soils*. International Journal of Heat and Mass Transfer, 2023. **206**: p.
757 123923.
- 758 80. Yang, Y., et al., *In situ methodology for thermal performance evaluation of building wall: A*
759 *review*. International Journal of Thermal Sciences, 2022. **181**: p. 107687.
- 760 81. d'Ambrosio Alfano, F.R., B.I. Palella, and G. Riccio, *Moisture in historical buildings from causes*
761 *to the application of specific diagnostic methodologies*. Journal of Cultural Heritage, 2023. **61**:
762 p. 150-159.
- 763 82. Liu, G., Y. Tan, and X. Li, *China's policies of building green retrofit: A state-of-the-art overview*.
764 Building and Environment, 2020. **169**: p. 106554.
- 765 83. Wu, D., et al., *Uncertainty analysis of envelope retrofits for existing residential buildings in*
766 *underdeveloped areas: A case study of Daokou, China*. Energy and Buildings, 2023. **284**: p.
767 112828.
- 768 84. Software, B., *Degree Days.net*. <https://www.degreedays.net/>, 2005.
- 769 85. Bo, R., et al., *Overheating of residential buildings in the severe cold and cold regions of China:*
770 *The gap between building policy and performance*. Building and Environment, 2022. **225**: p.
771 109601.
- 772